ELSEVIER

2 September 1996

PHYSICS LETTERS A

Physics Letters A 220 (1996) 149–157

Phase transformations in solid C_{60} at high-pressure–high-temperature treatment and the structure of 3D polymerized fullerites

V.D. Blank [a,b], S.G. Buga [a,b], N.R. Serebryanaya [a,b], G.A. Dubitsky [a], S.N. Sulyanov [a,c], M.Yu. Popov [a,b], V.N. Denisov [b], A.N. Ivlev [b], B.N. Mavrin [b]

[a] *Research Center for Superhard Materials, Centralnaya 7a, Troitsk, Moscow Region 142092, Russian Federation*

[b] *Institute of Spectroscopy of the Russian Academy of Sciences, Troitsk, Moscow Region 142092, Russian Federation*

[c] *Shubnikov Institute of Crystallography, Russian Academy of Sciences, Leninski Prospekt 59, Moscow 117333, Russian Federation*

Received 23 May 1996; accepted for publication 6 June 1996
Communicated by V.M. Agranovich

Abstract

New data concerning the solid C_{60} phase transformations in the pressure–temperature range $P = 6.5–13$ GPa, $T = 300–2100$ K and nonhydrostatic conditions are presented and plotted in the $P–T$ coordinates. The structure of superhard and ultrahard carbon phases obtained with these conditions is investigated by X-ray powder diffractometry and Raman scattering. New crystal structures of distorted bcc type and transient to diamond states are revealed in the synthesized samples. Fragments of different lengths of polymerized fullerene cages are found from resonance Raman spectra of the samples obtained at $P = 13$ GPa and $T < 1200$ K.

1. Introduction

The development of the original method for high-pressure–high-temperature treatment of solid C_{60} allowed us to create new superhard and ultrahard (harder than diamond) fullerite materials [1,2]. In these publications we reported the results of the first investigations of the structure and physical properties of the solid C_{60} specimens quenched after the nonhydrostatic pressure and heat treatment at $9.5 \leqslant P \leqslant 13$ GPa and $300 \leqslant T \leqslant 1830$ K. The volume of the synthesized samples was up to 40 mm^3. They are stable in oxidizers, and the structure of the hardest samples is stable at ambient conditions and at heating up to 1000 K in the air. Three types of the hardest materials were found, crystalline and amorphous, distinguished by their X-ray diffraction patterns and the Raman spectra. We suppose that the structures and properties of materials synthesized at high-pressure–high-temperature conditions and in the shear diamond anvil cell (SDAC) [3] at room temperature but at higher pressure are close, or that these materials are close to the states obtained earlier in the usual diamond anvil cells, described in Refs. [4–6] and some other publications. We assume that according to different high pressure, high temperature and shear deformation conditions the molecules in our samples either create 3D polymers with crystalline and amorphous structures or a cellular nanostructure of sp^2- and sp^3-hybridized carbon atoms.

PII S0375-9601(96)00483-5

It should be noted that neither the samples obtained in SDAC, nor the bulk superhard and ultrahard samples did include both diamond and the so-called "collapsed fullerite" carbon state [7]. The other carbon states obtained by Hirai et al. in shocked C_{60} fullerite and defined by them as "amorphous sp^3 nucleation" state and "new amorphous diamond" [8,9] have features similar to our amorphous ultrahard fullerites in the structure and physical properties, but some essential differences are discussed below. The set of new metastable crystal C_{60} phases discussed in Refs. [10,11] was synthesized under pressures in the range 2–5.5 GPa and at high temperatures. However, they are not hard, because strong covalent intermolecular bonds create only two-dimensional polymerization in the revealed phases, and the interlayer interaction at these structures is still of van der Waals-type, like in pristine C_{60} or in graphite. The existence of a superhard metastable state on the basis of partly coalescent C_{60} molecules at $P = 9.5$ GPa and $T = 620$–770 K was confirmed in Ref. [12].

The goal of the present study is a detailed investigation of the structures of the new fullerite samples and searching for the P–T-conditions of the fullerite–diamond transformation using the same experimental technique as in Refs. [1,2]. For these purposes the investigated pressure–temperature range was expanded to $P = 6.5$–13 GPa, $T = 300$–2100 K. The C_{60}-phases and other revealed carbon forms are plotted in the P–T coordinates of their formation areas.

We have used commercially available fcc C_{60} (99.8%; 0.1% C_{70}), manufactured at the Institute of Metal-Organic Chemistry, Nizhnij Novgorod, Russia. Dimensions of the synthesized samples were up to $\varnothing 4 \times 3$ mm^3. The time of heating under pressure was 1 min.

2. X-ray diffraction study

The structure of the quenched samples was studied by the X-ray powder diffraction method. The X-ray diffractometer KARD-6 with a flat proportional chamber on fast delay lines [13] was used. The accuracy of the Bragg angular determination was 0.01°. The Cu K_α radiation and graphite monochromator were applied. The diffraction patterns were obtained from small bits of the samples with 250–300 μm dimensions. During the exposition specimens were rotated to provide a better intensity averaging over the individual crystallites.

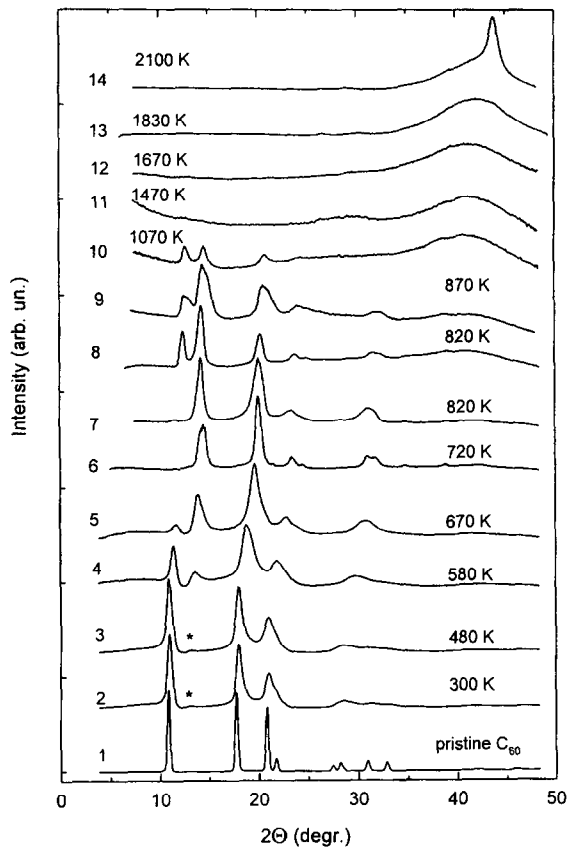

Fig. 1. Sequence of X-ray diffraction patterns of C_{60} fullerite quenched from 13 GPa and temperatures 300–2100 K; the asterisk indicates the peak of the polymerized phase.

Two types of states were found for the fullerite samples quenched after heat treatment at different temperatures: the crystalline states and the disordered or amorphous states. Fig. 1 shows the X-ray diffraction patterns of the samples obtained at different temperatures and at $P = 13$ GPa. This row clearly illustrates the alteration of crystal structure with the increase of synthesis temperature. The diffraction peaks are broader than the instrumental resolution function.

First we shall discuss the crystalline structure and phase transitions in the 300–1070 K range (Fig. 1, patterns nos. 1–10). After the pressure treatment at

300 K, the additional reflection (pattern no. 2), marked by the asterisk, appeared. This one does not belong to the pristine fcc structure because the cubic cell parameter, obtained from this line as (200), is 0.6 Å less than the value determined from the rest reflections. We suppose that this reflection is the strongest one of the new phase. It may be noted that the d-value of this reflection equals 6.72 Å at room temperature of the synthesis and equals 6.46 Å at 670 K. These values coincide with those of the two-fold and the five-fold diameters of the C_{60} molecule. The appearance of this reflection may be explained by the pressure induced orientational transition with the spin "freezing" and further polymerization of C_{60} molecules along their two-fold and five-fold axes.

At 580 K the diffraction pattern (no. 4) becomes generally two-phased. Earlier at 9.5 GPa [2] we have found that this temperature is a borderline which divides the formation areas of soft and hard samples of quenched fullerite. The inverse dependence of the cubic parameter a and the unit-cell volume V versus synthesis temperature T was found at a pressure of 13 GPa (Fig. 2) and at 9.5 GPa [2]. The numbers of the points in Fig. 2 correspond to the numbers of the diffraction patterns in Fig. 1. The temperature dependence of V for new crystal structures differs from

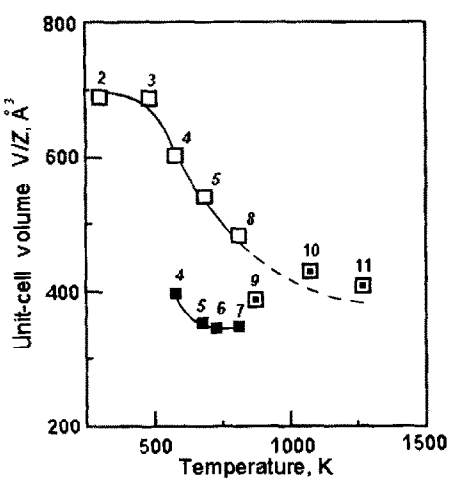

Fig. 2. Dependence of the unit-cell volume V on the synthesis temperature T for C_{60} phases quenched from 13 GPa pressure. The numbers correspond to the patterns in Fig. 1. (□) fcc structure; (■) distorted bcc structures; (⊡) monoclinic phases.

$V(T)$ for fcc phases. The distorted bcc phase is the densest one at 800 K. Then V increases with the increase of T and these structures transform to the monoclinic ones with a larger volume V.

The different diffraction patterns of new phases are present in Fig. 1, nos. 6–8. The crystal structure of sample no. 6 quenched from 720 K is proposed to be the orthorhombic pseudo-tetragonal body-centered one with the unit-cell parameters: $a = 9.53 \pm 0.06$ Å, $b = 8.87 \pm 0.04$ Å, $c = 8.34 \pm 0.03$ Å, $Z = 2$ (two C_{60} molecules). The indexing was done by the program DICVOL [14]. This structure is probably a distorted variant of the bcc structure [15], where the central molecule might be rotated round a two-fold axis with respect to molecules placed at the corners. In connection with this fact and the orthorhombic distortion the unit cell is primitive, which was confirmed by the indexing. The density, calculated from X-ray data, is equal to 3.39 g/cm^3. The experimental density obtained by the hydrostatic weighting method is equal to 3.2 ± 0.1 g/cm^3. The measured value is lower than the calculated one due to the presence of less dense phases and defects in the studied sample. It is possible to represent the parameters of this structure on the basis of the fcc parameter a_{cub}: $a = a_{cub}/\sqrt{2} + \Delta$, $b = a_{cub}/\sqrt{2}$, $c = a_{cub}/\sqrt{2} - \Delta$, where $\Delta = 0.6$ Å and $a_{cub} = 12.6$ Å. The transformation probably takes place along face diagonals of the fcc structure [110]. Assuming that the shape of the molecule has not changed at polymerization, we have found the C–C bond length to be equal to 1.53 Å in the [111] direction of the orthorhombic structure and in the three-fold axis directions of C_{60} molecules. This state exists in the narrow temperature interval 670–720 K.

The samples obtained at a temperature of 820 K consist of two phases with different crystal structures. Their diffraction patterns are nos. 7, 8. Comparing pattern no. 7 with pattern no. 6 we have noted a broadening of the peaks and the appearance of the additional reflection $d = 7.6$ Å. This is not the same reflection as at the lower temperature (nos. 2, 3) and it does not correspond to a small quantity of the fcc structure with the other parameter because the fcc structure is not indexed from the other lines. We propose the more distorted orthorhombic crystal structure to describe these patterns. The unit-cell parameters, obtained by DICVOL for the patterns

registered on different parts of the same sample are: $a = 11.16$–11.22 Å, $b = 8.17$–9.05 Å, $c = 7.58$–7.68 Å, $Z = 2$. The X-ray densities of these structures are equal to 3.08–3.4 g/cm^3. The experimental densities were 2.95–3.2 g/cm^3. It should be noted that the value of the X-ray density for the fcc structure with $a = 12.2$ Å, obtained for the same conditions (no. 8) is equal to 2.6 g/cm^3. Thus, the measured values of the density prove the idea of transformation to the proposed orthorhombic structure. Assuming again absence of distortions in the shape of the molecules, we have calculated the intermolecular distance as 1.455 Å along the space diagonal of the orthorhombic structure. In this direction, the C_{60} molecules are oriented along their two-fold or five-fold axes. The distance between the molecules along the [001] axis of the structure is equal to 1.5 Å, and the C_{60} molecules are combined together along their three-fold axis. Therefore, the description of the structure within the framework of nondeformed molecules and their definite orientation during the polymerization process allow us to explain the distortions of the body-centered cubic structure. This experimental fact may be considered as evidence that 3D polymerization takes place in the samples, and it does not cause an essential deformation of the C_{60} molecules in the structure. This conclusion should be noted particularly in comparison with the 5% deformation of the molecules in the case of 2D polymerization [10,16].

Diffraction pattern no. 8 shows that for the same conditions as when the new orthorhombic crystal structure was obtained, the fcc type structure still exists. We may assume that this structure is the compressed variant of a simple cubic one by analogy with the low-pressure orientational transformations [17], but the difference in the diffraction patterns of fcc and sc structures can be observed only in the case of a perfect crystal structure, which we obviously do not have. The unit-cell parameter of this structure is 12.4–12.2 Å and it decreases with an increase of the synthesis temperature. The (200) reflection is the strongest one, probably because some quantity of the orthorhombic structure is present. In the two-phased samples the orthorhombic structure is getting more disordered, which is expressed by the broadening and the extension of the peak shape towards larger scattering angles. With an increase of the synthesis temperature, the intensities of the (111) and (200) reflections become equal and strongest. It is important to note that if this structure with $a = 12.3$ Å would differ from the fcc structure described in Ref. [10] with $a = 13.6$ Å only by some scaling factor, then the (111) reflection should be absent according to the molecular form factor [4]. The existence of the strong (111) reflection in pattern no. 8 probably confirms that C_{60}-molecules do not rotate freely and the shape of the molecules is distorted due to polymerization. With an increase of temperature, the diffraction patterns (nos. 9, 10) become more and more disordered and diffuse, and a halo at 2.16–2.18 Å appears. We suggest that the new cubic structures are distorted into a monoclinic one (no. 9) with the following parameters: $a = 8.77$ Å; $b = 12.48$ Å; $c = 7.59$ Å; $\beta = 110.6°$, $Z = 2$, $\rho_{X\text{-ray}} = 3.07$ g/cm^3. The experimental density of the samples is 3.1 ± 0.1 g/cm^3. At synthesis temperatures above 1000 K the crystalline part of the diffraction patterns decreases while the intensity of the reflections from the amorphous phase grows. Since the crystalline part of diffraction pattern no. 10 is very poor, it was not possible to perform the indexing. Ignoring reflection splitting we are able to index the crystalline part of this pattern approximately as a cubic structure with $a = 12.1 \pm 0.1$ Å from three broad diffuse peaks (111), (200), (220). The intensity of the (111) reflection is almost equal to the intensity of (200), and the (220) intensity decreases sharply. Finally, there are only haloes on the patterns of the samples obtained above 1300 K.

As noted earlier [2], the crystalline state of C_{60} fullerite stays up to the synthesis temperature 1270 K if samples are treated at 13 GPa, while at 9.5 GPa the crystalline state exists up to 750 K only.

The annealing of the samples obtained at $T = 820$ K and $P = 13$ GPa was investigated at different temperatures in the range 300–1270 K during 1 hour in the sealed quartz tube. The crystal structure stayed up to 900 K heating, then it transformed into an amorphous carbon state. The relatively low heat stability of the studied crystal structure probably means the existence of highly active unsaturated double carbon bonds in it.

Patterns nos. 10–14 show the formation of the disordered carbon states from solid C_{60} at $P = 13$ GPa, $T > 1000$ K, when a strong halo occurs with a maximum at the d spacing 2.18–2.16 Å. The inten-

sity of the halo increases with an increase of T and the following diffuse maxima registered by photomethod appear at 1.25 and 1.08 Å d spacing. Indications for the 3.3 Å halo are also present, but it is much less intense. The pattern obtained with the sample quenched from 1830 K shows that the band at 2.16 Å becomes asymmetric and pattern no. 14 exhibits the appearance of a wide line at 2.06 Å. This line should be attributed to the formation of the diamond-like structure. However, the haloes at 2.18–2.16 Å, 1.25 Å and 1.08 Å probably originate from the carbon hexagons. This will be discussed in Section 4.

3. Raman scattering data

The Raman spectra were studied by means of a multichannel spectrometer [2,3] using excitation with the 457.9 and 632.8 nm lines at a grazing incidence of laser beams. The power density did not exceed 50 W/cm^2 for the hard samples ($T > 600$ K) and 10 W/cm^2 for the soft samples ($T < 600$ K). Let us discuss the Raman spectra excited with the 457.9 nm line.

The spectra of fullerite samples change with an increase of the synthesis temperature (Fig. 3). At $T < 600$ K the spectra still preserve the main features of pristine fullerite although they show a band broadening and redistribution of relative intensities of Raman bands. In particular, as in the case of fullerite in the diamond anvil cell [3], the intensity of the "pentagonal pinch" mode near 1468 cm^{-1} essentially decreases with increasing temperature. Besides, a new band appears at 930–950 cm^{-1}. We have observed this band earlier [2] in the Raman spectra of fullerite samples synthesized at 9.5 GPa. This band was assigned to stretch vibrations of four-member carbon rings forming between molecules at polymerization of 2 + 2 cycloaddition type. Although this band has been always seen in the Raman spectra when dimers [18] or chains [19] of fullerene molecules are formed, it was, however, absent in the first-principle calculations of polymerized C_{60} [20]. The Raman bands of the fullerite samples synthesized at 13 GPa and room temperature are essentially broader than those in pristine fullerite. Moreover, bandwidths broaden with increasing synthesis temperature. As we shall show below, this broadening is inhomogeneous.

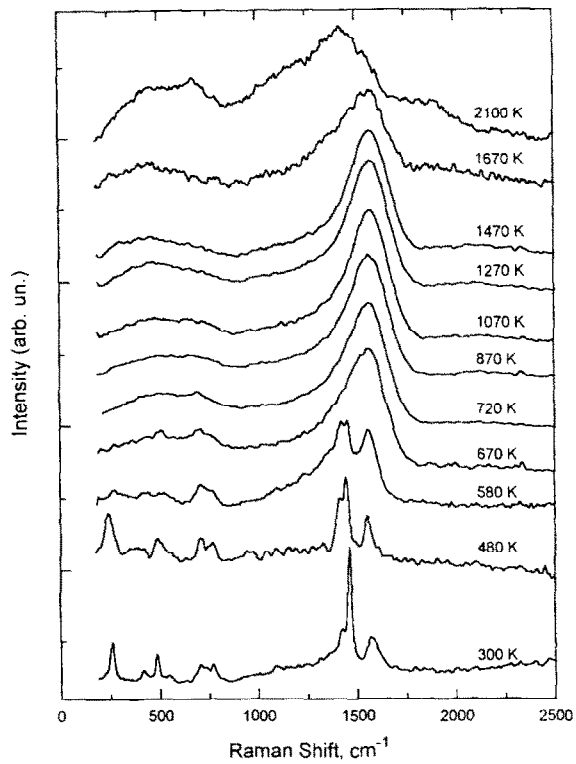

Fig. 3. Raman spectra of fullerite quenched from 13 GPa and the different temperatures; excitation with the 457.9 nm lines.

At $T > 600$ K the Raman spectra obtain some new features. One of them is the single broad band at $\omega > 1000$ cm^{-1}. The change of the Raman spectra at $T \approx 600$ K agrees with the X-ray data assuming structural phase transitions and "freezing" the rotation of the molecules due to the formation of covalent intermolecular bonds at this temperature. At $T > 600$ K the shape of the spectra changes slightly with temperature increase up to $T \approx 1500$ K. Only a small shift of the Raman band from 1560 to 1570 cm^{-1} was observed.

At $T > 1500$ K new bands near 1350 and 1900 cm^{-1} appear. At $T = 2100$ K the intensity of these bands becomes stronger and the 1570 cm^{-1} band shifts to lower frequencies down to 1425 cm^{-1}. The appearance of the 1900 cm^{-1} band can be due to a collapse of fullerene cages. It is known that this band appears in the Raman spectra of carbon structures if allene-type fragments (C=C=C) form. We assign

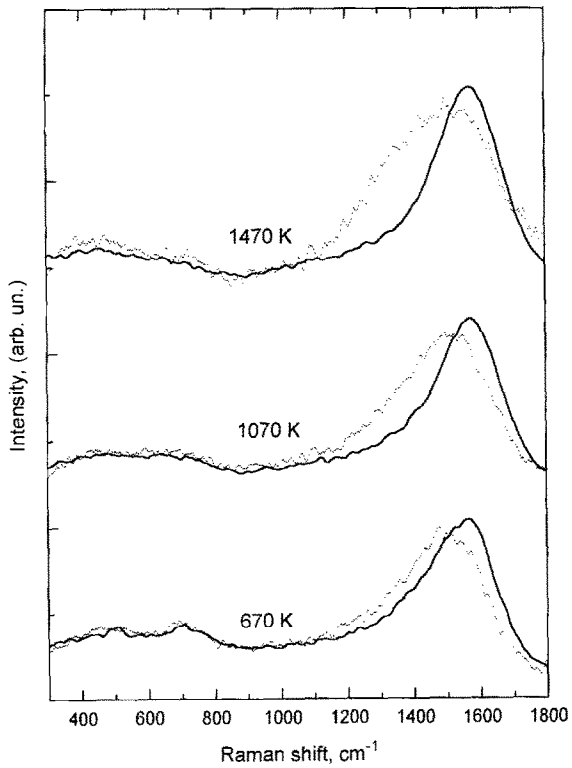

Fig. 4. Dependence of the Raman spectra of fullerite quenched from 13 GPa and the different excitation temperatures; solid lines: 457.9 nm; points: 632.8 nm.

the 1350 cm^{-1} band to the formation of diamond microcrystals, which is also consistent with the X-ray data.

Now let us compare the Raman spectra obtained at 457.9 and 632.8 nm excitations. Fig. 4 shows that the high-frequency band near 1550 cm^{-1} experiences an essential low-frequency shift from 1562 cm^{-1} at 457.9 nm to 1480 cm^{-1} at 632.8 nm for 670 K and from 1570 to 1490 cm^{-1} for 1070 and 1470 K. The dependence of the band frequencies on the excitation wavelengths is, probably, due to a strong inhomogeneity of the samples. Such a situation is known for polymers containing various lengths of chains. An increase of the chain length results in a decrease of the mode frequencies and a shift of the electronic absorption band to low energies [21]. Therefore, both the resonance conditions for the Raman scattering and mode frequencies differ for short and long chains. Analogous with polymers, we assume that our samples have various lengths of chains (or fragments) of polymerized fullerene cages. At the 632.8 nm excitation there is a resonance enhancement of the Raman intensity for long chains (fragments), but for short chains (fragments) it is at 457.9 nm. At the 457.9 nm excitation the width of the 1570 cm^{-1} band changes slightly with increasing temperature (Figs. 3 and 4). However, we observe an essential broadening of the corresponding band at the 632.8 nm excitation (Fig. 4). We consider that this is due to the fact that a disorder, increasing with temperature, should manifest itself more strongly in spectra of long fragments than in spectra of short fragments.

4. *P–T* regions of phases

4.1. Crystal structures

The areas of the purest observed fullerite states and other carbon forms are plotted in Fig. 5 according to their synthesis conditions. The regions of different quenched crystal structures are presented in the lower part of the diagram. At a pressure of 6.5 and 7.5 GPa we obtained rhombohedral phases like in Ref. [10], and at 8 GPa denser modification was observed. Different symbols denote different types of fcc, distorted bcc and monoclynic C_{60} fullerite structures, which were discussed in Section 2.

4.2. Amorphous I type fullerite state

The central part of the diagram shows the *P–T* region for the synthesis of the first amorphous (am.1) type state. We have presented the X-ray, the Raman and the TEM data concerning the structure of this state in Refs. [1,2]. Since the experimental parameters *c* are equal to the diameters of the C_{60} molecule, 6.7, 6.5 and 6.2 Å, we suppose that these structures may be 3D-polymers of sp^3-bonded molecules. The coalescence of the molecules discussed in Ref. [12] takes place probably at higher temperatures and long heating time. At temperatures $T > 1300$ K a certain part of them is destroyed, but this process ends probably at much higher temperatures (Fig. 1).

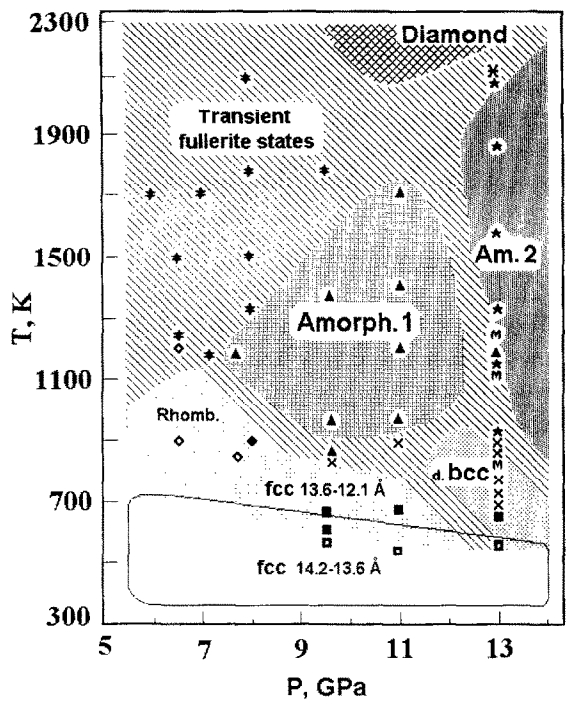

Fig. 5. $P-T$ regions of quenched C_{60}-phases and the other carbon structures obtained by high-pressure–high-temperature synthesis. The structures denoted in the diagram are discussed in the text. Symbols are experimental points obtained by us and by other authors.

4.3. Transient fullerite states

The region shaded by inclined lines represents two-(or more)-phased states of C_{60} or more complicated transient fullerite states between the areas of the homogeneous states of C_{60} and other carbon forms.

The samples obtained at the $P-T$ conditions corresponding to the upper left part of the diagram have diffraction patterns and the Raman spectra similar to turbostrate graphite [2]. But the structure of these samples has to differ from graphite because their hardness is 40–70 GPa. This material may be considered as superhard. Perhaps C_{60} molecules destroyed at these $P-T$ conditions form a carbon hexagon net, "bridges", between unbroken molecules. It would be appropriate to call this intermediate state "graphite-like fullerite". Probably, similar structures were revealed earlier [22], but their hardness is up to 40 GPa and that does not allow us to consider these materials as superhard.

4.4. Diamond

Our synthesis conditions occur in the stability region of diamond [23]. That is why the transformation of C_{60} into diamond is more likely than into graphite at our $P-T$ conditions. When we used the ordinary catalyst, an almost 100% transformation of fullerite to diamond was obtained at $P = 8$ GPa, $T = 1800$ K. But according to the X-ray diffraction patterns (Fig. 1), and the Raman spectra (Fig. 3), solid C_{60} transforms into diamond structure only at $T \geqslant 2000$ K approximately. We consider the "diamond" denoted in the right upper corner of the diagram as a nanosize diamond [24] or a type of the "new amorphous diamond" [9].

4.5. Amorphous 2 fullerite state

Another amorphous carbon structure (am.2) synthesized from C_{60} [2] is shown at the right side of the diagram. In Ref. [2] we found the 2.1 Å d-spacing by the X-ray pattern for this state. The present study allowed us to determine the position of the halo maximum as 2.18–2.16 Å. Although this value corresponds to the d-spacing of hexagonal diamond (lonsdalite) [24], we can not identify the obtained carbon state as lonsdalite because of the absence of splitting into peaks at 2.06 and 1.96 Å, which should be present for lonsdalite. The exception is pattern no. 14 in Fig. 1, but this sample should be considered as a mixture of the am.2 state with diamond.

We assume that a d-spacing of 2.16–2.18 Å corresponds to the (100) peak from the carbon hexagons with the parameter $a = 2.50 \pm 0.01$ Å. In the case when the hexagonal nets are connected by covalent sp^3-bonds without long-range order along the c-axis, the diffraction pattern of this structure consists of the $hk0$ peaks [25]. The calculated d-spacings from $a = 2.50$ Å for the reflections (100), (110) and (200) are the following: 2.16, 1.25 and 1.08 Å, which we have found experimentally [2]. If we accept that the parameter c equals 6.67–6.19 Å (Fig. 1, no. 11), then the calculated X-ray density of this carbon structure is 3.0–3.4 g/cm^3. This density is consistent with our experimental values 3.1–3.4 g/cm^3 for the amorphous samples obtained at 13 GPa. When we suppose am.2 is a mixed sp^2–sp^3-state with a cage nanostructure then one can estimate the

interatomic distances (Å): 1.50 ± 0.02, 2.50 ± 0.02, 3.10 ± 0.02, 3.80 ± 0.05 and 6.7 ± 0.1. These distances were found from the radial distribution function $G(r)$ of the shocked C_{60} fullerite samples [9]. However, that $G(r)$ was attributed to the pure sp^3-bonded state called new amorphous diamond. Excluding the fullerene-originated values 3.10 and 6.8 Å, the same interatomic distances were obtained from the experimentally determined [26] and simulated [27] $G(r)$ of the amorphous diamond-like films produced by ion beam deposition (i-C). It is known that films of this type are not homogeneous, the ratio between sp^3- and sp^2-bonds is usually not better than 80% and 20% and the hardness for i-C may exceed diamond hardness. Actually, in Ref. [27] it is claimed that the mixed sp^3- and sp^2-bonded structure may be more rigid than the pure sp^3-bonded diamond in the case of an appropriate relation between the quantities of these bonds. That may be the reason for the ultrahard properties of the am.2 state [2]. We suppose that the hardness of the am.2 state may be higher than the i-C hardness due to a higher density and the cage structure.

In Refs. [9,28] the 2.2 and 1.2 Å d-spacings of shocked C_{60} were assigned to another pure sp^3-bonded amorphous diamond by analogy with e-C (evaporated amorphous carbon), which has similar d-values. But e-C is rather a graphite-like than a diamond-like material and its density is usually less than 2.5 g/cm^3. The X-ray density calculated from $d_{111} = 2.2$ Å for the diamond structure is less than 3.0 g/cm^3, whereas the experimental value was higher than 3.3 g/cm^3. It was noted that this amorphous diamond was similar to collapsed fullerite [7]. However, collapsed fullerite had neither X-ray reflections nor Raman scattering. The absence of the Raman scattering was explained by the complete sp^3-bonding of carbon. On the other hand, the amorphous ultrahard fullerite (am.2) has quite definite Raman spectra (Fig. 3, $720 < T < 1470$ K) and broad X-ray bands displaying the existence of sp^2-bonds.

One should note that the density of the am.2 state is close to the calculated density 3.35 g/cm^3 of the quenched state [29] found from the simulation of compressing C_{60} molecules to 4.4 g/cm^3 and heating to 2500 K. The sp^3–sp^2-bonds ratio was calculated to be 79% and 21%, respectively. Besides, the calculated $G(r)$, up to $r = 5$ Å, for the simulated collapsed C_{60} [29] coincides with the calculated and experimentally determined $G(r)$ of i-C [26,27]. Probably the structure of the nearest atomic environment in the am.2 state is similar to i-C, whereas its nanoscale structure contains the molecular and intermolecular cages that are absent in i-C.

5. Conclusion

We have found that new crystalline and amorphous carbon structures are formed from fullerite quenched after high-pressure–high-temperature treatment in a wide P–T region. Transient fullerite states containing two or more phases are detected between the areas of the monostructural states. P–T regions for the formation of these structures are built.

For the first time the bcc structure of fullerite was found at 13 GPa. Traces of this structure appear at room temperature, gradually increase with temperature, distorting at high temperature to a monoclinic structure. The crystalline structures are stable at heating up to 900 K.

We have found three amorphous states of quenched fullerite: the am.1 and am.2 states and "graphite-like fullerite" (transient state), which are different by their properties. All of them contain sp^2- and sp^3-bonds. Their properties and nanostructure depend on the sp^3–sp^2-ratio. We suppose that the structure of the am.1 state may be a 3D polymer of sp^3-bonded C_{60} molecules. The hardest phase, called ultrahard fullerites (the am.2 state), contains an essential quantity of sp^2-bonds and, probably, has a carcass nanostructure.

Acknowledgement

This work was partly supported by the National Foundation for Intellectual Collaboration (Grant No. 95076) and the National Foundation for Basic Research (Grant No. 96-02-16322a). We are grateful to E.E. Semenova and V.V. Aksenenkov for the assistance in the experiments.

References

[1] V. Blank, S. Buga, M. Popov, V. Davydov, G.. Dubitskij, B. Kulnitskij, E. Tatyanin, V. Agafonov, R. Ceolin, H. Szwarc

and A. Rassat, Abstracts of XXXII Annual Meeting of the European high pressure research group, Brno, Czech Republic, August 1994, p. 31;
V.D. Blank et al., Phys. Lett. A 204 (1995) 151.
[2] V.D. Blank et al., Phys. Lett. A 205 (1995) 208; Mol. Mat. 7 (1996) 251.
[3] V.D. Blank, S.G. Buga, M.Yu. Popov, V.A. Davydov, V.N. Denisov, A.N. Ivlev, B.N. Mavrin V. Agafonov, R. Ceolin, H. Szwarc and A. Rassat, Phys. Lett. A 188 (1994) 281.; V.D. Blank et al., Mol. Mat. 4 (1994) 149.; V.D. Blank et al., New J. Chem. 19 (1995) 2532.
[4] S.J. Duclos, K. Brister, R.C. Haddon, A.F. Kortan and F.A. Thiel, Nature 351 (1991) 380.
[5] D.W. Snoke, Y.S. Raptis and K. Syassen, Phys. Rev. B 45 (1992) 14419;
C.S. Yoo and W.J. Nellis, Chem. Phys. Lett. 198 (1992) 379.
[6] J.H. Nguyen, B.M. Kruger and R. Jeanloz, Solid State Commun. 88 (1993) 719.
[7] F. Moshary et al., Phys. Rev. Lett. 69 (1992) 466;
S.D. Kosowsky et al., Phys. Rev. B 48 (1993) 8474.
[8] H. Hirai and K. Kondo, Phys. Rev. B 51 (1995) 15555.
[9] H. Hirai, Y. Tabira, K. Kondo, T. Oikawa and N. Ishizawa, Phys. Rev. B 52 (1995) 6162.
[10] Y. Iwasa et al., Science 264 (1994) 1570.
[11] J-L. Hodeau, J.M. Tonneree, B. Bouchet-Fabre, M. Nunez Regueiro, J.J. Capponi and M. Perroux, Phys. Rev. B 50 (1994) 10311;
M. Nunez Regueiro, L. Marques, J-L. Hodeau, O. Bethoux and M. Perroux, Phys. Rev. Lett. 74 (1995) 278;
I.O. Bashkin et al., J. Phys. Condens. Matter 6 (1994) 7491.
[12] B. Keita, L. Nadjo, V. Davydov, V. Agafonov, R. Ceolin and H. Szwarc, New. J. Chem. 19 (1995) 769.
[13] S.A. Sulyanov, A.N. Popov and D.M. Kheiker, J. Appl. Cryst. 27 (1994) 934.
[14] A. Boultif and D. Louer J. Appl. Cryst. 24 (1991) 987.
[15] M. O'Keeffe, Nature 352 (1991) 674.
[16] G. Oslanyi and L. Forro, Solid State Commun. 93 (1995) 265.
[17] A. Lundin and B. Sundqvist, Europhys. Lett. 18 (1994) 463.
[18] B. Burger, J. Winter and H. Kuzmany, Z. Phys. B, in press.
[19] M.C. Martin et al., Phys. Rev. B 51 (1995) 3210.
[20] G.B. Adams, J.B. Page, O.F. Sankey and M. O'Keeffe, Phys. Rev. B 50 (1994) 17471.
[21] E. Mulazzi, G.P. Brivio, E. Faulques and S. Lefrant, Solid State Commun. 46 (1983) 851.
[22] M.E. Kozlov, M. Hirabayashi, K. Nozaki, M. Tokumoto and H. Ihara, Appl. Phys. Lett. 66 (1995) 1199;
A. Kokorevics, J. Gravitis and J. Kalnacs, Chem. Phys. Lett. 243 (1995) 205.
[23] H. Kanda and T. Sekine, Properties and growth of diamond, EMIS Data Rev. Series No. 9 (1994) 404.
[24] G.A. Adadurov et al., Neorganicheskie Materialu 13 (1977) 649.
[25] A.V. Kurdyumov and A.N. Pilyankevich, Phase transformations in carbon and boron nitride (Naukova Dumka, Kiev, 1979).
[26] P.H. Gaskell, A. Saeed, P. Chieux and D.R. Mckenzie, Phys. Rev. Lett. 67 (1991) 1286.
[27] P.C. Kelires, Phys. Rev. B 47 (1993) 1829.
[28] H. Hirai, K. Kondo, N. Yoshizawa and M. Shiraishi, Appl. Phys. Lett. 64 (1994) 1797;
V.V. Brazhkin et al., Pisma, Zh. Eksp. Teen. Fiz. 62 (1995) 328.
[29] B.L. Zhang, C.Z. Wang, K.M. Ho and C.T. Chan, Europhys. Lett. 28 (1994) 219.